Analyst

Accepted Manuscript

ROYAL SOCIETY OF CHEMISTRY

www.rsc.org/analyst

Cite this: DOI: 10.1039/c0xx00000x

www.rsc.org/xxxxxx

PAPER

Mixed hydrogel bead-based tumor spheroid formation and anticancer drug testing

Yaolei Wang,[a] and Jinyi Wang*[a,b]

Received (in XXX, XXX) Xth XXXXXXXXX 20XX, Accepted Xth XXXXXXXXX 20XX

DOI: 10.1039/b000000x

Three-dimension multicellular tumor spheroids have become a critical object for anticancer study since they may provide a better model than conventional monolayer culture of cancer cells. Various methods for tumor spheroid formation have been explored. However, only one kind of hydrogel was used in these methods, which has an influence on the size and morphology of the obtained tumor spheroids. Herein, we presented a microfluidic droplet-based method for the formation of multicellular tumor spheroids using alginate and matrigel mixed hydrogel beads. By on-chip changing the flow rate of the two hydrogel solutions, mixed hydrogel beads with different volume ratios between alginate and matrigel were obtained. Meanwhile, human cervicalcarcinoma (HeLa) cells were encapsulated in the mixed hydrogel beads. Acridine orange and propidium iodide double-staining assay showed that the viability of cells encapsulated in the the mixed hydrogel beads was more than 90%. After 4 day culture, the multicellular tumor spheroids were successfully formed with spherical shape and uniform size distribution compared with spheroids formed in pure alginate beads. Cytoskeletal analysis by TRITC-phalloidin staining showed that HeLa cells in the mixed hydrogel beads closely linked to each other. The dose-dependent response assay of HeLa cell spheroids to vincristine showed that multicellular spheroids had more powerful resistance to vincristine compared to conventional monolayer culture cells. Taken together, this novel technology may be of importance to facilitate *in vitro* culture of tumor spheroids for their ever-increasing utilization in modern cell-based medicine.

Introduction

Majority of cells in the body experience a three-dimensional (3D) environment provided by neighboring cells and extracellular matrix (ECM).[1] Although, *in vitro* study, with the advantages of well-controlling the cell environment, facilitating microscopic analysis and medium changes, and sustaining cell proliferation for most cell types, cell monolayers cultured on flat substrates is still widely used, it fail to recapitulate the architecture of living tissues.[2] To overcome the disadvantages in two-dimensional (2D) cell culture, researchers have attempted to develop efficient 3D cell culture systems. Among these systems, the simplest and most feasible 3D cell culture method was multicellular spheroid culture, which has been chosen as a culture model to mimic and study 3D cell structures.[3] Since the 3D *in vitro* model of avascular solid tumor was constructed in 1980 by using multicellular spheroids (MCSs),[4] the MCSs embedded in ECM-like gels have been used to investigate the mechanisms of tumor cell invasion.[5] The MCS-based assay represents a promising alternative that not only overcomes the disadvantages of 2D cell culture, but also builds a bridge between cell-based and animal-based studies.

MCSs can be formed by using conventional methods, such as the hanging drop method,[6-8] gyratory rotation,[9,10] and liquid overlay culture.[11] However, these methods suffered from some disadvantages such as cell damage due to shear stress, low yield and the difficulty in controlling MCS size.[12,13] To overcome these challenges, recently, micro-manufacturing technologies, such as microarrays,[14] microwells,[15] and microfluidic devices[16] have been used to form MCSs. Among these micro-manufacturing technologies, microfluidic droplet-based cell encapsulation in 3D hydrogel beads has obtained more attentions because it offers several advantages: 1) the rapid and high-throughput generation of cell-loaded hydrogel beads allows to reduce labor;[17] 2) the miniaturized cell culture in microbeads allows efficient transport of oxygen, nutrients, and metabolites to ensure cell viability;[18] and 3) hydrogel matrix with different permeability can be used to adjust hydrogel bead property to protect cells from host's immune response, which may eliminate the need of immunosuppressive drugs and improve transplantation outcome.[12] To date, several microfluidic droplet-based methods have been developed for cell encapsulation in hydrogel by using synthetic or natural polymers, such as alginate, agrose, gelatin, and poly(ethylene glycol) and its derivatives.[19-23] However, in these studies, only one kind of polymer was used to produce cell-loaded hydrogel beads. Because of the intrinsic property of a single polymer, these methods always met a problem that solid-like hydrogel core of beads leads to the formation of cell aggregates with uncontrollable size and shape.[13] The use of

multicomponent polymers in hydrogel beads for MCS formation is enticing: properties of one component can compensate for disadvantages of another, while the advantages of each individual component can be simultaneously reserved.[24] In addition, the properties of multicomponent hydrogels, such as chemical composition, porosity, stiffness, elasticity, structural integrity, and cell adhesion, can be tuned by varying the concentrations of each component.[25,26] Although mixtures of hydrogels have been used as 2D substrates for cell culturing and scaffolds for tissue engineering,[27-29] very few of them were use to study 3D cell culture in a microenvironment. The possible reason may be that there is not a suitable method for continuous mixing and on-line tuning the composition of hydrogel during cell encapsulating for MCS formation.

In this study, we presented a microfluidic droplet system for cancer cell spheroid formation in a mixed hydrogel bead. Two kinds of hydrogels were utilized in this system. One is alginate, the other is matrigel. Alginate is a block copolymer which cross-links in the presence of divalent cations such as Ca^{2+}.[30] Because of its biodegradability, rapid solidification using calcium ions, and high permeability to nutrients, alginate is a widely used material for cell spheroid study.[31,32] Matrigel is a natural basement membrane matrix obtained from Engelbreth-Holm-Swarm mouse sarcoma, and is a mixture of various proteins including growth factors and ECM proteins such as laminin and collagen, which stays liquid at 4 °C but self-assembles into a gel when incubated at 37 °C.[33] The different hardening process characteristic of matrigel improves the final morphological characteristics of the mixed hydrogel beads obtained. Moreover, cancer cells encapsulated in mixed hydrogel beads can digest matrigel so that eliminate the effect of the solid core of hydrogel bead on the size and shape of cell aggregates.[34] By on-chip tuning the composition of alginate and matrigel using this microfluidic droplet system, we successfully obtained human cervicalcarcinoma cell spheroids with high cellular viability and uniform size in the mixed hydrogel beads. To further illustrate the cell spheroids formed in the mixed hydrogel beads have the ability to mimic the properties of tumors, their change in cytoskeletal structure was analyzed and anticancer drug testing against these cell spheroids were performed using vincristine.

Experimental

Materials and reagents

RTV 615 polydimethylsiloxane (PDMS) prepolymer (RTV 615 A) and curing agent (RTV 615 B) were purchased from Momentive Performance Materials (Waterford, NY, USA). The surface-oxidized silicon wafers were obtained from Shanghai Xiangjing Electronic Technology Ltd. (Shanghai, China). The AZ 50XT photoresist and developer were bought from AZ Electronic Materials (Somerville, NJ, USA). Acridine orange (AO), propidium iodide (PI), Hoechst 33258, Sodium alginate, M8410 mineral oil and sorbitan monooleate (SPAN 80) were purchased from Sigma-Aldrich (MO, USA). Matrigel matrix was obtained from BD Biosciences (Franklin, NJ, USA). Vincristine was purchased from Haizheng Pharmaceutical Co., Ltd. (Zhejiang, China). The Dulbecco's Modified Eagle Medium (DMEM) with high glucose, fetal bovine serum (FBS), trypsin, and TRITC-phalloidin were obtained from Gibco Invitrogen Corporation (CA, USA). All solvents and other chemicals were purchased from local commercial suppliers and were of analytical reagent grade, unless otherwise stated. All solutions were prepared using ultrapurified water supplied by a Milli-Q system (Millipore).

PDMS microfluidic device fabrication

The microfluidic device used in this study was fabricated using soft lithography with PDMS.[35] Briefly, microscale patterns used for droplet production were first created using AutoCAD 2008 (Autodesk, USA) and printed at a resolution of 20,000 dots per inch (DPI) on a transparency film (MicroCAD Photomask Ltd., Suzhou, China) to be used as the photomask. Then, a mould with 30 μm high features was fabricated in a single step under UV light using an AZ 50XT photoresist on a BG-401A mask aligner (7 mW cm^{-2}, CETC, China).

To fabricate the PDMS microfluidic device, the mould was first exposed to chlorotrimethylsilane (Alfa Aesar, Lancs, England) vapor for three minutes to promote elastomer release after carrying out the baking steps.[36] A mixture of PDMS [RTV 615 A and B (10 : 1, w/w)] was then poured onto the mould to yield a 3 mm-thick fluidic layer. After degassing, the mould was baked for 30 min at 85 °C. Then, the PDMS flow layer structure was peeled from the mould. Through-holes were punched with a metal pin at the terminals of the inlet and outlet channels. Next, the fluidic layer was placed on top of a glass slide (2500 rpm, 45 s, ramp 15 s) coated with a thin PDMS film [RTV 615 A and B (5 : 1)] that was cured for 20 min in an oven at 80 °C. The microfluidic device was then ready for use after baking at 80 °C for 48 h.

Cell culture

Human cervicalcarcinoma (HeLa) cells were obtained from the Chinese Academy of Sciences (Shanghai, China). The cells were cultured using DMEM supplemented with 10% FBS, 100 U mL^{-1} penicillin, and 100 μg mL^{-1} streptomycin in a humidified atmosphere of 5% CO_2 at 37 °C. The cells were normally passaged at a ratio of 1:2 every 3 days to maintain them in the exponential growth phase. When the cells reached confluence, they were harvested through trypsinization with 0.25 wt % trypsin in phosphate buffered solution (PBS, 0.01 M, pH 7.4) at 37 °C. Trypsinization was stopped by adding freshly supplemented DMEM. The cell suspension was centrifuged at 1000 rpm for 3 min. The cells were then resuspended in supplemented DMEM for further use.

Mixed hydrogel bead formation and cell encapsulation

The cell suspension was prepared at a concentration of 1×10^7 cell mL^{-1} using DMEM mixed with 50% (v/v) matrigel at 4 °C. Sodium alginate (2 wt %) in DMEM was filtered with a 0.22 μm syringe filter (Millex-GV, Millipore) to remove any clumps of alginate.[21] The 4 wt % $CaCl_2$ in DMEM and mineral oil with 5 wt % SPAN80 were also filtered with a 0.22 μm syringe filter for sterilization. For droplet formation, the dispersed phases consisted of cell suspension and alginate in DMEM. Mineral oil was used as an immiscible solvent and 5 wt % SPAN 80 was added to stabilize the droplets.[37] All solutions were injected into the microfluidic channel using a syringe pump (LSP01-1A, Baoding Longer Precision Pump Co., Ltd., Hebei, China). By

using a 50 cm long Teflon tube (ID 0.3 mm and OD 0.7 mm), the droplets were collected externally in a $CaCl_2$ bath and gelled. After gelation, the gelled hydrogel beads were washed with PBS, centrifuged at 300 rpm and placed into DMEM in a 35 mm cell culture dish (Nunc, Denmark). The cell encapsulated hydrogel beads were cultured in a humidified atmosphere of 5% CO_2 at 37 °C for 6 days and the medium was changed everyday.

Cell spheroid-based antitumor drug test

To conduct antitumor drug test against the cancer cell spheroids, vincristine[38] was chose as the antitumor drug in the present study. After spheroids formation, the drug-free culture media was replaced with 0, 1, 2, 5, or 10 μM vincristine in DMEM. Control groups of normal 2D monolayer cultured cells were treated with the same concentrations of vincristine after reaching 60% to 80% confluence, the standard for *in vitro* cell analyses, particularly for quantitative assessment of cell activity.[39] After 24 h treatment, cell viability was assessed using a common AO/PI staining protocol.[40]

Cell staining

Cell viability assessment was performed using a common AO/PI staining protocol.[40] Following by removing the growth medium and washing with PBS carefully, the AO/PI staining solution (10 μg mL^{-1} each in PBS) was introduced into the plates and the staining process was performed for 10 min at room temperature. Then, PBS was introduced for 10 min as a final rinse. F-actin of cells was stained with TRITC-phalloidin to visually investigate cellular interaction and cytoskeleton structure of cell spheroids.[41] Briefly, the cell spheroids were fixed using 4% paraformaldehyde for 10 min at room temperature after washing thrice with PBS. Then, the cell spheroids were permeabilized with PBS containing 0.2% Triton X-100 for 30 min and incubated at 37 °C for 20 min with TRITC-phalloidin (100 nM in PBS). The cell nuclei were stained with H33258 fluorochrome (0.5 μg mL^{-1} in PBS) for 10 min.[42]

Microscopy and image analysis

Phase-contrast and fluorescence images of cells were obtained using an inverted microscope (Olympus, CKX41) with a charge-coupled device camera (Olympus, DP72) and a mercury lamp (Olympus, U-RFLT50). Confocal Laser Scanning Microscopy (CLSM) images were acquired with an Olympus FV 1000 confocal microscope. The image and data analyses were performed using Image-Pro® Plus 6.0 (Media Cyternetics, Silver Spring, MD) and SPSS 12.0 (SPSS Inc.), respectively. The results, including the error bars in the graphs, were given as the mean ± standard deviation.

Results and discussion

Design of the microfluidic device

An overview together with a schematic illustration of the design of the microfluidic device is shown in Figs. 1a-c. The PDMS chip is functionally composed of two parts: one is for scattering cells and the other is for droplet formation (Fig. 1b). The cell scattering part consists of a 5-loop curved microchannel (50 μm width, 30 μm height, and 100 μm spatial interval) and one inlet for the introduction of cell and matrigel mixture. After passing through the curved microchannel, affecting by the Dean force cell-encapsulated droplets were separated.[42] The droplet formation part was composed of an oil channel (100 μm width and 30 μm height), two separate side channels (50 μm width and 30 μm height) for alginate flow, three inlets and one outlet. The cell supension was caught in the middle by two alginate flows (Fig. 1c). The oil and aqueous solutions meet at a cross junction and spontaneously generate a droplet due to their different interfacial properties.[43] Inlets and outlet in the device were used for loading, purging and removing processes.

Mixed hydrogel bead generation and cell encapsulation

To generate the mixed hydrogel beads in the microfluidic device, 50% (v/v) matrigel in DMEM either with or without HeLa cells, 2 wt % sodium alginate in DMEM, and mineral oil were injected into the microdevice through the curved, side, and oil channels, respectively. Similar to previous studies,[44,45]droplets with tunable and uniform sizes were generated using this system (Fig. 2a-c). By changing the flow rate of oil and aqueous phase, the diameter of droplets ranged from 44 ± 2.63 μm to 406 ± 10.16 μm (Fig. 2d). To test the ability of forming droplets with different concentration of fluorescein, fluorescein (100 μM fluorescein in $NaHCO_3$ buffer, pH 8.3) was injected into the device through the curved channels. At the same time, fresh $NaHCO_3$ buffer was injected into the two side channels and mineral oil was injected into the oil inlet at a flow rate of 1.5 μL min^{-1}. The total flow rate of aqueous phases (V_1+2V_2, V_1 is the flow rate of fluorescein and V_2 is the flow rate of $NaHCO_3$ buffer) was maintained at 0.75 μL min^{-1}. As shown in Fig. 3a, fluorescein flow was caught in the middle by two buffer flows. The lower ratio of V_1: $2V_2$, the narrower the fluorescein flow was (Fig. 3b). As a result, the concentration of formed fluorescein droplets decreased proportionately (Fig. 3c). These results demonstrated that by changing the flow rate ratio of two aqueous phases, different concentrations of fluorescein droplets can be easily formed. Therefore, the microfluidic device can be used to formed mixed hydrogel droplets with different volume ratios of alginate and matrigel.

The morphological and dimensional characteristics of hydrogel beads play a crucial role in the formation of cell spheroids.[1] One of the most vital influence factors to the morphology of hydrogel beads is the composition of hydrogel.[28] Thus, to find out the optimal volume ratio of alginate and matrigel for generating mixed hydrogel beads with spherical shape, different ratios between alginate and matrigel were tried in the current study. As shown in Fig. 4a, the hydrogel beads of pure alginate were characterized by a tailed-shape. This particular shape was attributed to the slow passing of the alginate liquid droplets through the oil phase/gelling bath interface.[46] To obtain spherical hydrogel beads for cancer cell spheroid formation, we conducted subsequent experiments using alginate/matrigel blend dispersions as water phases, with the purpose to facilitate droplet passage through the oil phase/gelling bath interface by partly gelling the droplets before collecting them into the $CaCl_2$ bath. As mentioned above, matrigel stays liquid at 4 °C but self-assembles into a gel at 37°C.[33] To make sure the gelation of matrigel occurred before the alginate gelling, a 50 cm long Teflon tube (ID 0.3 mm and OD 0.7 mm) that was put in 37 °C water was connected to the device outlet. Analysis of the microphotographs (Fig. 4b-c)

showed that the progressively increasing of matrigel results in an improvement of the final morphology of the mixed hydrogel beads. However, as the volume ratio between matrigel and alginate exceeded 1:1, the morphology of the mixed hydrogel beads became irregular (Fig 4d). As a result, the volume ratio between matrigel and alginate was determined as 1:1 to form mixed hydrogel beads in the subsequent experiments. The optimal flow rates for the formation of stable hydrogel beads were 0.375 μL min^{-1} for cell/matrigel channel, 0.19 μL min^{-1} for each of the two alginate channels, and 1.5 μL min^{-1} for oil channel. Under this condition, hundreds of spherical hydrogel beads containing HeLa cells were obtained (Fig. 4e). The diameter of the mixed hydrogel beads was 254±15.3 μm and ~ 80% of the hydrogel beads had a diameter ranging from 250 μm to 270 μm (n =100) (Fig. 4f).

Culture of HeLa cells in mixed hydrogel beads

In this study, mixed hydrogel beads containing a few tens of HeLa cells were generated (Fig. 5a). Live/dead cell staining assay[40] showed that the viability of HeLa cells was 94.67 ± 1.48% (Fig. 5d), which indicated that neither shear through the device nor exposure to mineral oil and calcium bath was harmful to cells. To test the capabilities of our approach for cell spheroid formation, we monitored the fate of encapsulated cells for several days in standard culture conditions. Images of the encapsulated HeLa cells at 0, 24, 48, and 96 h demonstrating their proliferation are shown in Fig. 5a. Initially, HeLa cells were randomly distributed throughout the mixed hydrogel beads. As time passed, the sparse cells in the hydrogel beads became denser and more compact. After 96 h culture, cells merged to form a single spheroid in the hydrogel bead with high cell viability (Fig. 5a). The diameter of the spheroid itself in the mixed hydrogel bead was about 138 ± 20 μm. HeLa cells were also encapsulated in pure alginate beads as the control group. As shown in Fig. 5b, cells became denser and more compact as days passed, similar to cells cultured in the mixed hydrogel. The viability of HeLa cells encapsulated in pure alginate beads during culture time (0-96 h) was more than 94%, which was almost the same with HeLa cells encapsulated in mixed hydrogel beads (Fig. 5d). However, as described above, pure alginate beads had a tailed-shape so that cells encapsulated in alginate beads proliferated along the tail, resulting in the formation of non-spheroid shape of cell aggregates (Fig. 5b). Moreover, comparing with those cells encapsulated in microcapsules, [47,48] cells encapsulated in mixed hydrogel beads are closer to the cells *in vivo*. Because in natural microenvironments, all cells, except the circulating ones, require anchorage to a matrix.[49] The gelled alginate in the mixed hydrogel beads provide the matrix for cells. In addition, matrigel played a crucial role that ECM played *in vivo* in the mixed hydrogel beads.

Cytoskeleton analysis

To visually observe the cell-cell connection in the cell spheroids formed in the mixed hydrogel beads, cytoskeleton of cells in the cell spheroids was stained with TRITC-phalloidin, a chemical that can bind to F-actin of cells,[42] after 5 days culture (Fig. 5c). The nuclei of cells were stained with H33258 fluorochrome. The results showed that in the mixed hydrogel beads cells attached each other without empty gaps and the cell spheroids was formed, however, in the pure alginate beads there were gaps between cells and the shape of cell aggregates were irregular. These results illustrated that in mixed hydrogel beads HeLa cells could digested matrigel to form a 3D cell-to-cell direct contact. However, in the control group the direct cell-cell connection was inhibited by the solid core of pure alginate beads. Moreover, the tailed-shape of alginate beads influenced the shape of cell aggregates. These results were consistent with previous observation, i.e., solid-like hydrogel core would lead to the formation of cell aggregates with uncontrollable size and shape.[13]

Cell spheroid-based antitumor drug test

Cancer cells respond differently to drugs when cultured in flasks as compared to 3D culture.[32] Because of the ability to effectively mimic the properties of a tumor, cancer cell spheroids were always used for cancer-related studies such as anticancer drug screening.[50] Different from typical 2D cells, 3D multicellular spheroids have high proliferation rate and strong drug resistivity.[51] To confirm these features of the mixed hydrogel-based cell spheroids, an antitumor drug (vincristine) was chosen for the analysis. Vincristine, which belongs to a kind of cell cycle specific agent, is generally a mitotic inhibitor because it irreversibly binds to microtubules and spindle proteins in mitotic S-phase. Thus, vincristine interferes with mitotic spindle assembly and further inhibits tumor cell development.[52] HeLa cells, a general choice for solid tumor research, were used in this study because of their frequent appearance in clinical tumor investigations.[53]

HeLa cells were treated with different concentrations of vincristine for 24 h after 6 day culture. Images of AO/PI staining were used to determine cell viability and proliferation of the multicellular spheroids. In each case, the cell response within the mixed hydrogel beads was compared with those in a standard monolayer culture. One of the problems in comparing the results of antitumor drug tests from multicellular spheroids and those from monolayer culture is that the use of the live/dead staining-based cell viability analysis may undercount the number of dead cells in the monolayer culture. After treatment with anticancer drugs, dead cells usually detach from the culture surface and are removed during the pipetting of the staining solutions, which results in high cell viability due to undercounting the dead cells.[54] To prevent this situation occurred, in this study all the cells were first removed from the culture flask using trypsin/EDTA. The entire suspension containing both live and dead cells was then stained, centrifuged and imaged. The results of 24 h vincristine treatment show that the drug concentration usedis negatively related to the change of cell viability (Fig. 6). Low concentration (1 μM and 2 μM) treatment made cell spheroid growth slow and high vincristine concentrations (5 μM and 10 μM) showed obvious influence on both cell viability and proliferation rate of the cell spheroids. However, there was no obvious diameter decrease observed (Fig. 6c). This was probably because of short-time (24 h) drug treatment. In addition, most of the dead cells in the mixed hydrogel beads were found on the outer layer of the cell spheroids, indicating that only cells in the outer layer were mainly affected by the antitumor drug, which is a feature commonly found in multicellular tumors.[3,21] Moreover, the results also demonstrated that HeLa cell spheroids had more resistance to vincristine than those cells grown in monolayer culture (Fig.

6d). In the monolayer culture (2D model) and the mixed hydrogel beads (3D model), HeLa cell viability all decreased with the increase in vincristine concentration. However, HeLa cells in the mixed hydrogel beads had higher viability than those in culture flask. The higher concentration of vincristine the more obvious phenomenon was found. This phenomenon is probably caused by the 3D architecture of cell spheroids that increased cell-cell contact or tight packing, which might hinder the penetration or diffusion of drugs into the spheroids. These results are in a good correspondence with previously observations, i.e., spheroid-bounded cells are less sensitive to anticancer agents than monolayer cultured cells.[55] This is one of the reasons for motivating studies on three-dimensional tumor models.

Conclusions

In summary, we successfully fabricated a microfluidic droplet device for cell spheroid generation by using alginate and matrigel mixed hydrogen. Combined with the conventional protocol used for alginate bead formation, cell-encapsulated mixed hydrogel beads were successfully obtained. The results showed that the volume ratio between alginate and matrigel in the hydrogel beads can be adjusted by changing the flow rate of the two hydrogel solutions. The mixed hydrogel beads were demonstrated to be excellent for the formation of HeLa cell spheroid compared to the pure alginate bead. Anticancer drug test showed that cancer cell spheroids formed in the mixed hydrogel beads had the ability to mimic the properties of tumors. These results indicated that the microfluidic device might be an efficiently tool for the preparation of multicellular tumor spheroids, which could be used in a variety of cancer studies such as cell-cell interactions, oncotherapy, and high-throughput screening of anticancer drug.

Acknowledgments

This study was supported by the National Natural Science Foundation of China (21175107 and 21375106), the Ministry of Education of the People's Republic of China (NCET-08-602 0464), the Scientific Research Foundation for the Returned Overseas Chinese Scholars, the State Education Ministry, and the Northwest A&F University.

Notes and references

[a] *College of Science, Northwest A&F University, Yangling, Shaanxi, 712100, China. Tel: +86-298-708-2520; E-mail: jywang@nwsuaf.edu.cn*
[b] *College of Veterinary Medicine, Northwest A&F University, Yangling, Shaanxi, 712100, China*

1 K. Alessandri, B. R. Sarangi, V. V. Gurchenkov, B. Sinha, T. R. Kießling, L. Fetler, F. Rico, S. Scheuring, C. Lamaze, A. Simon, S. Geraldo, D. Vignjevic, H. Doméjean, L. Rolland, A. Funfak, J. Bibette, N. Bremond and P. Nassoy, *Proc. Natl. Acad. Sci. U. S. A.*, 2013, **110**, 14843-14848.
2 E. Cukierman, R. Pankov, D. R. Stevens and K. M. Yamada. *Science*, 2001, **294**, 1708-1712.
3 R.-Z. Lin and H. Y. Chang, *Biotechnol. J.*, 2008, **3**, 1172-1184.
4 R. M. Sutherland. *Science*, 1988, **240**, 177-184.
5 G. Y. Lee, P. A. Kenny, E. H. Lee and M. J. Bissell. *Nat. Methods*, 2007, **4**, 359-365.
6 S. L. Nyberg, B. Amot, U. A. Arquikar, R. P. Remmel and P. Rinaldo, *Liver Transplant.*, 2005, **11**, 901-910.
7 M. Ingram, G. B. Techy, R. Saroufeem, O. Yazan, K. S. Narayan, T. J. Goodwin and G. F. Spaulding, *In Vitro Cell. Dev. Biol.: Anim.*, 1997, **33**, 459-466.
8 J. B. Kim, R. Stein and M. J. O'Hare, *Breast Cancer Res. Treat*, 2004, **85**, 281-291.
9 R. L. Carpenedo, C. Y. Sargent and T. C. McDevitt, *Stem Cells*, 2007, **25**, 2224-2234.
10 P. Manley and P. I. Lelkes, *J. Biotechnol*, 2006, **125**, 416-424.
11 S. Sakai, S. Ito and K. Kawakami, *Acta Biomater.*, 2010, **6**, 3132-3137.
12 W. Zhang, S. Zhao, W. Rao, J. Snyder, J. K. Choi, J. Wang, I. A. Khan, N. B. Saleh, P. J. Mohler, J. Yu, T. J. Hund, C. Tang and X. He, *J. Mater Chem B Mater Biol Med*, 2013, **2013**, 1002-1009.
13 J. L. Wilson and T. C. McDevitt, *Biotechnol Bioeng*, 2013, **110**, 667-682.
14 M. Y. Lee, R. A. Kumar, S. M. Sukumaran, M. G. Hogg, D. S. Clark and J. S. Dordick, *Proc. Natl. Acad. Sci. U.S.A.*, 2008, **105**, 59-63.
15 K. H. Lee, da Y. No, S. H. Kim, J. H. Ryoo, S. F. Wong and S. H. Lee, *Lab Chip*, 2011, **11**, 1168-1173.
16 M. C. Chen, M. Gupta and K. C. Cheung, *Biomed Microdevices*, 2010, **12**, 647-654.
17 D. Velasco, E. Tumarkin and E. Kumacheva, *Small*, 2012, **8**, 1633-1642.
18 M. Serra, C. Correia, R. Malpique, C. Brito, J. Jensen, P. Bjorquist, M. J. Carrondo and P. M. Alves, *PLoS One*, 2011, **6**, e23212.
19 S. Sakai, S. Ito, H. Inagaki, K. Hirose, T. Matsuyama, M. Taya and K. Kawakami, *Biomicrofluidics*, 2011, **5**, 013402-013407.
20 E. Tumarkin, L. Tzadu, E. Csaszar, M. Seo, H. Zhang, A. Lee, R. Peerani, K. Purpura , P. W. Zandstra and E. Kumacheva, *Integr. Biol.*, 2011, **3**, 653-662.
21 S. Yoon, J. A. Kim, S. H. Lee, M. Kim and T. H. Park, *Lab Chip*, 2013, **13**, 1522-1528.
22 A. Kumachev, J. Greener, E. Tumarkin, E. Eiser, P. W. Zandstra and E. Kumacheva, *Biomaterials*, 2011, **32**, 1477-1483.
23 D. Steinhilber, S. Seiffert, J. A. Heyman, F. Paulus, D. A. Weitz and R. Haag, *Biomaterials*, 2011, **32**, 1311-1316.
24 A. Batorsky, J. Liao, A. W. Lund, G. E. Plopper and J. P. Stegemann, *Biotechnol. Bioeng.*, 2005, **92**, 492-500.
25 A. W. Lund, J. A. Bush, G. E. Plopper and J. P. Stegemann, *J. Biomed. Mater. Res. Part B App. Biomat.*, 2008, **87**, 213-221.
26 Z. Chen, L. Wang and J. P. Stegemann, *J. Microencapsulation*, 2011, **28**, 344-352.
27 M. S. Shoichet, *Macromolecules*, 2010, **43**, 581-591.
28 L. Capretto, S. Mazzitelli, G. Luca and C. Nastruzzi, *Acta Biomater.* 2010, **6**, 429-435.
29 S. Sakai, I. Hashimoto and K. Kawakami, *Biotechnol. Lett.*, 2007, **29**, 731-735.
30 K. S. Huang, T. H. Lai and Y. C. Lin, *Lab Chip*, 2006, **6**, 954-957.
31 L. Yu, M. C. Chen and K. C. Cheung, *Lab Chip*, 2010, **10**, 2424-2432.
32 K. Y. Lee and D. J. Mooney, *Prog Polym Sci*, 2012, **37**, 106-126.
33 H. K. Kleinman and G. R. Martin, *Semin. Cancer Biol.*, 2005, **15**, 378-386.
34 D. M. Hall and S. A. Brooks, *Methods Mol. Biol.*, 2014, **1070**, 1-11.
35 L. Ren, W. Liu, Y. Wang, J. C. Wang, Q. Tu, J. Xu, R. Liu, S. F. Shen and J. Wang, *Anal. Chem.*, 2013, **85**, 235-244.
36 X. Huang, L. Li, Q. Tu, J. Wang, W. Liu, X. Wang, L. Ren and J. Wang, *Microfluid. Nanofluid.*, 2011, **10**, 1333-1341.
37 C. N. Baroud, F. Gallaire and R. Dangla, *Lab Chip*, 2010, **10**, 2032-2045.
38 X. Wang, F. Wei, A. Liu, L. Wang, J.C. Wang, L. Ren, W. Liu, Q. Tu, L. Li and J. Wang, *Biomaterials*, 2012, **33**, 3719-3732.
39 J. Wang, Z. Wan, W. Liu, L. Li, L. Ren, X. Q. Wang, P. Sun, L. L. Ren, H. Y. Zhao, Q. Tu, Z. Y. Zhang, N. Song and L. Zhang, *Biosens. Bioelectron.*, 2009, **25**, 721-727.
40 W. Liu, L. Li, J. C. Wang, Q. Tu, L. Ren, Y. Wang and J. Wang, *Lab Chip*, 2012, **12**, 1702-1709.
41 Y. J. Weng, W. W. Kuo, C. H. Kuo, K. C. Tung, C. H. Tsai, J. A. Lin, F. J. Tsai, D. J. Y. Hsieh, C. Y. Huang and J. M. Hwang, *Mol. Cell. Biochem.*, 2010, **345**, 241-247.

42 E. W. Kemna, R. M. Schoeman, F. Wolbers, I. Vermes, D. A. Weitz and A. van den Berg. *Lab Chip*, 2012, **16**, 2881-2887.

43 C. N. Baroud, F. Gallaire and R. Dangla, *Lab Chip*, 2010, **10**, 2032-2045.

44 J. Sha, Y. Wang, J. Wang, L. Ren, Q. Tu, W. Liu, X. Wang, A. Liu, L. Wang and J. Wang, *J. Biosci. Bioeng.*, 2011, **112**, 373-378.

45 J. Sha, Y. Wang, J. Wang, L. Ren, W. Liu, Q. Tu, A. Liu, L. Wang and J. Wang, *Analy. Method*, 2011, **3**, 1988-1994.

46 L. Capretto, S. Mazzitelli, C. Balestra, A. Tosi and C. Nastruzzi, *Lab Chip*, 2008, **8**, 617-621.

47 X. Wang, W. Wang, J. Ma, X. Guo, X. Yu and X. Ma, *Biotechnol Prog.*, 2006, **22**, 791-800.

48 S. Sakai, S. Ito, Y. Ogushi, I. Hashimoto, N. Hosoda, Y. Sawae and K. Kawakami, *Biomaterials*, 2009, **30**, 5937-5942.

49 G. Mehta, A. Y. Hsiao, M. Ingram, G. D. Luker and S. Takayama, *J. Control Release*, 2012, **164**, 192-204.

50 E. Gottfried, L. A. Kunz-Schughart, R. Andreesen and M. Kreutz, *Cell Cycle*, 2006, **5**, 691-695.

51 L. A. Kunz-Schughart, J. P. Freyer, F. Hofstaedter and R. Ebner, J. *Biomol. Screening*, 2004, **9**, 273-285.

52 X. Wang, F. Wei, A. Liu, L. Wang, J.C. Wang, L. Ren, W. Liu, Q. Tu, L. Li and J. Wang, *Biomaterials*, 2012, **33**, 3719-3732.

53 T. Nieto-Miguel, R. I. Fonteriz, L. Vay, C. Gajate, S. Lo´pez-Herna´ndez and F. Mollinedo, *Cancer Res.*, 2007, **67**, 10368-10378.

54 J. H. Sung and M. L. Shuler, *Lab Chip*, 2009, **9**, 1385-1394.

55 X. Zhang, W. Wang, W. Yu, Y. Xie, X. Zhang, Y. Zhang and X. Ma, *Biotechnol. Prog.*, 2005, **21**, 1289-1296.

Captions to Figures

Figure 1. Microfluidic flow-focusing device for the generation of mixed hydrogel droplets from two aqueous fluids: a) an overview of the microfluidic device with reference to a coin; b) a schematic view of the microchannel system: I-1, I-2, I-3 and I-4 are the inlets of cells, alginate, alginate and mineral oil flows, respectively, and O-1 is the outlet; c) a cartoon zoom-in look of the region for cell encapsulating, and d) typical images showing cells encapsulated in mixed hydrogel droplets. Scar bar is 30 μm.

Figure 2. Typical phase contrast images of droplet generation in the device with different sizes: a) 417 ± 4.77 μm, b) 226 ± 7.81 μm, and c) 122 ± 2.72 μm. Scar bar is 300 μm; d) show the relationship between Q_o/Q_w (Q_o is the flow rate of oil and Q_w is the flow rate of water) and the droplet size. Q_w was set as 0.25 μl min^{-1}, 0.375 μl min^{-1}, 0.5 μl min^{-1}, and 0.75 μl min^{-1}. As the increase of Q_o, droplet size decreased in all groups of Q_w. Different sizes of droplet can be formed from 44 ± 2.63 μm to 417 ± 4.77 μm.

Figure 3. Mixed aqueous droplets formed in the device using fluorescein. a) Observable fluorescence distribution in the channel at different flow ratios and the formed droplets. V_1 is the flow rate of the cell channel and V_2 is the flow rate of the side channel. The two side channels had the same flow rate. b) Quantitative concentration distribution in the channel (red arrow) at the different flow ratios. c) The normalization fluorescence concentration in the formed droplets. Scar bar is 80 μm.

Figure 4. Droplet-based mixed hydrogel bead formation and cell encapsulation. Typical phase contrast images of mixed hydrogel hydrogel beads with different volume ratio between alginate and matrigel: a) 1:0, b) 2:1, c) 1:1, and d) 1:2, respectively. Scar bar is 100 μm. e) HeLa cells encapsulated in the mixed (alginate: matrigel = 1:1, v/v) hydrogel beads. Scar bar is 200 μm. f) The diameter distribution of hydrogel droplets. The mean droplet diameter was 254 ± 15.3 μm (n = 100).

Figure 5. Time-sequence images of viability and proliferation of HeLa cells encapsulated in the a) mixed hydrogel (alginate: matrigel = 1:1) beads and b) pure alginate beads. The corresponding fluorescence image showing high viability (green) of the encapsulated HeLa cells both in the mixed and pure hydrogel beads. Scale bar is 75 μm. c) Fluorescence image of the cytoskeleton structure of the cultured HeLa cell spheroid in the mixed hydrogel bead (left) and pure alginate bead (right). Spheroids were stained with TRITC-phalloidin (red) and Hoechst (blue). Scale bar is 15 μm. d) Viability of cells in the mixed hydrogel beads and pure alginate beads.

Figure 6. a) Live/dead staining images of vincristine treated cell spheroids. Concentrations of 0, 1, 2, 5 and 10 μM vincristine were added to 6-day incubated cell spheroids. Scale bar is 50 μm. Cell viability was assayed after 24 h. Green and red fluorescence indicates viable cells and dead cells, respectively. b) Live/dead staining images of vincristine treated monolayer culture cells in control group. Vincristine was added after cell reaching 60% to 80% confluence. c) Images of HeLa cell spheroid proliferating before and after treatment with vincristine. d) Effects of vincristine concentration on cell viability in various culture environments. e) Proliferation of HeLa cell spheroids under different concentrations of vincristine. The growth rate was measured as $(S_a\text{-}S_b)/S_b$, where S is the total surface area of spheroids, a means after drug treatment and b means before drug treatment.

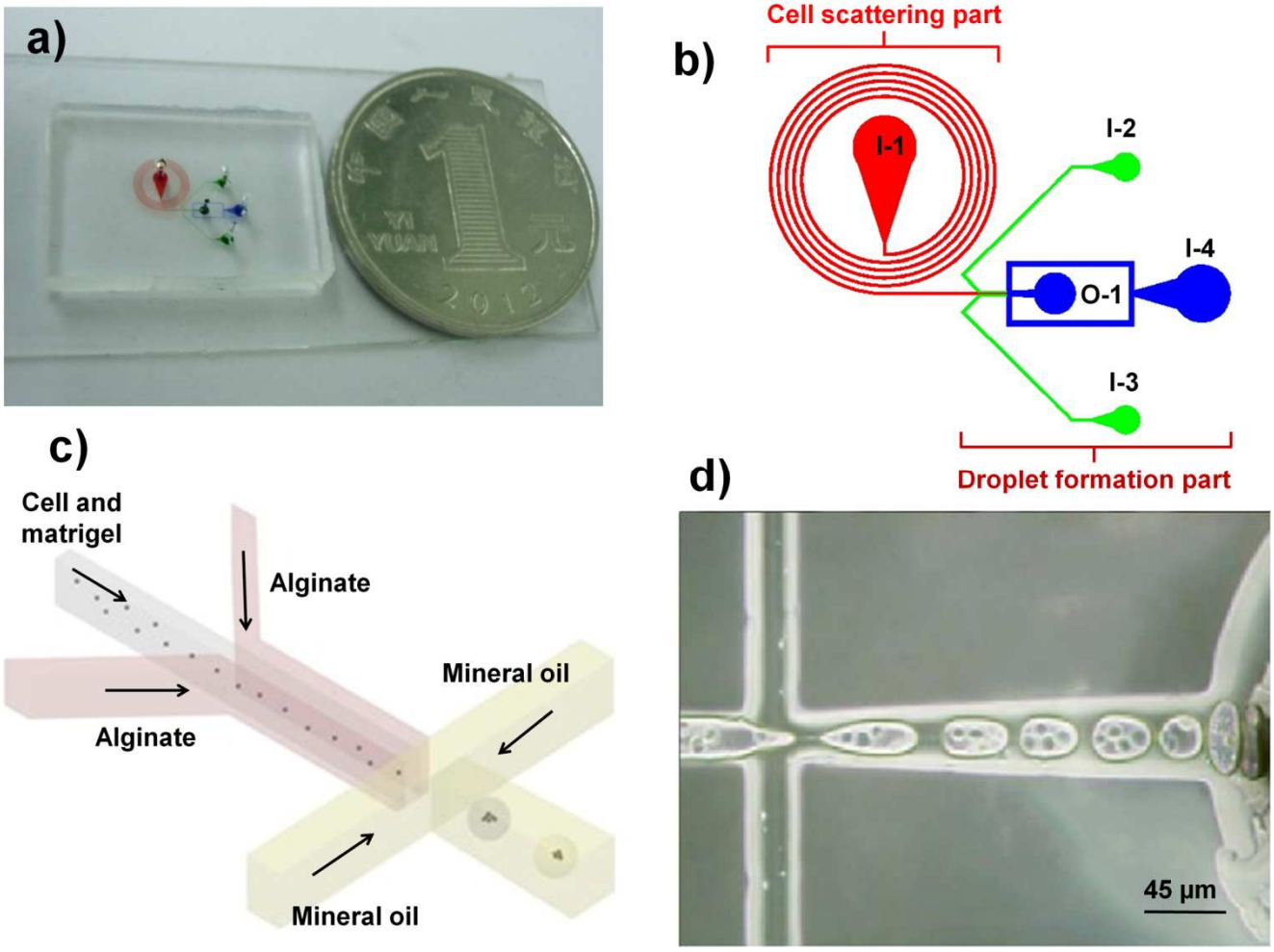

Fig. 1

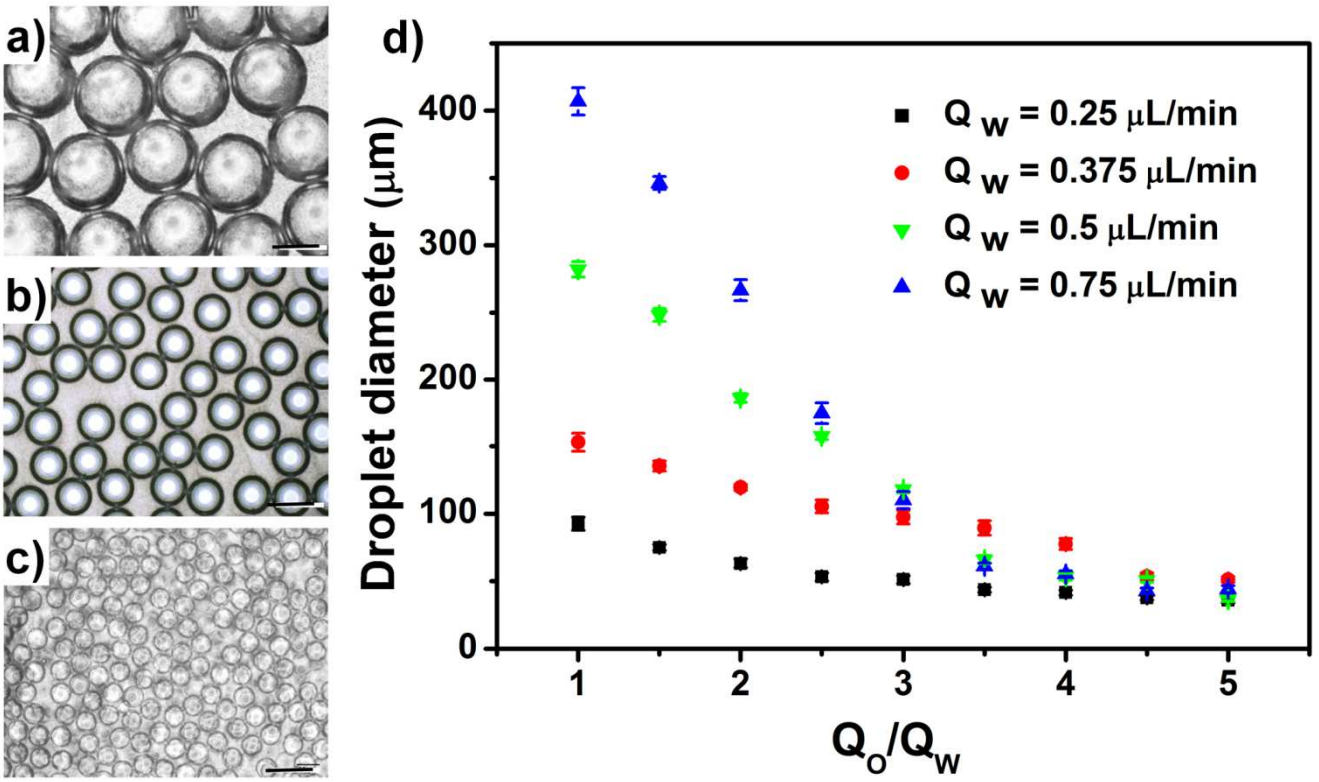

Fig. 2

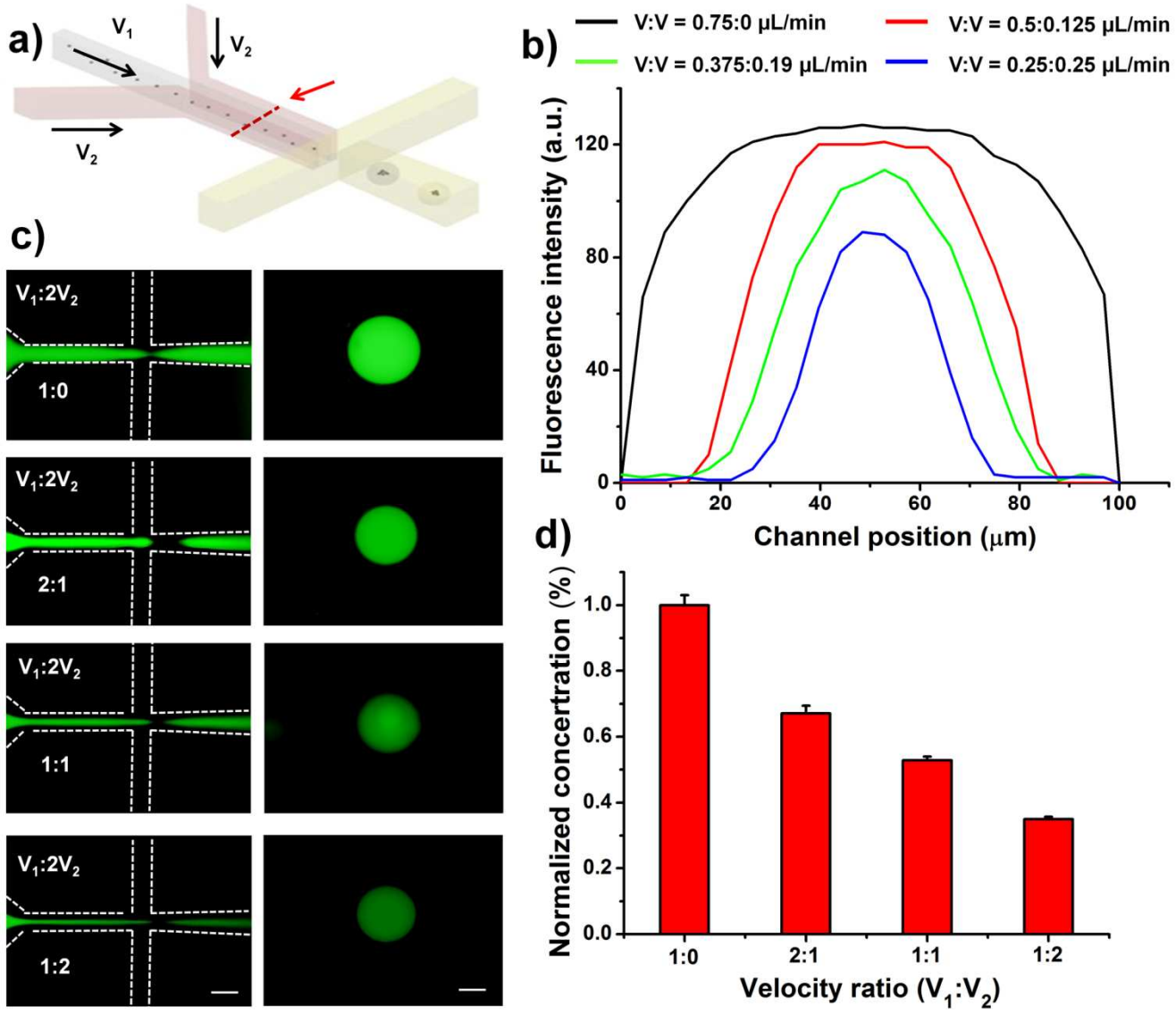

Fig. 3

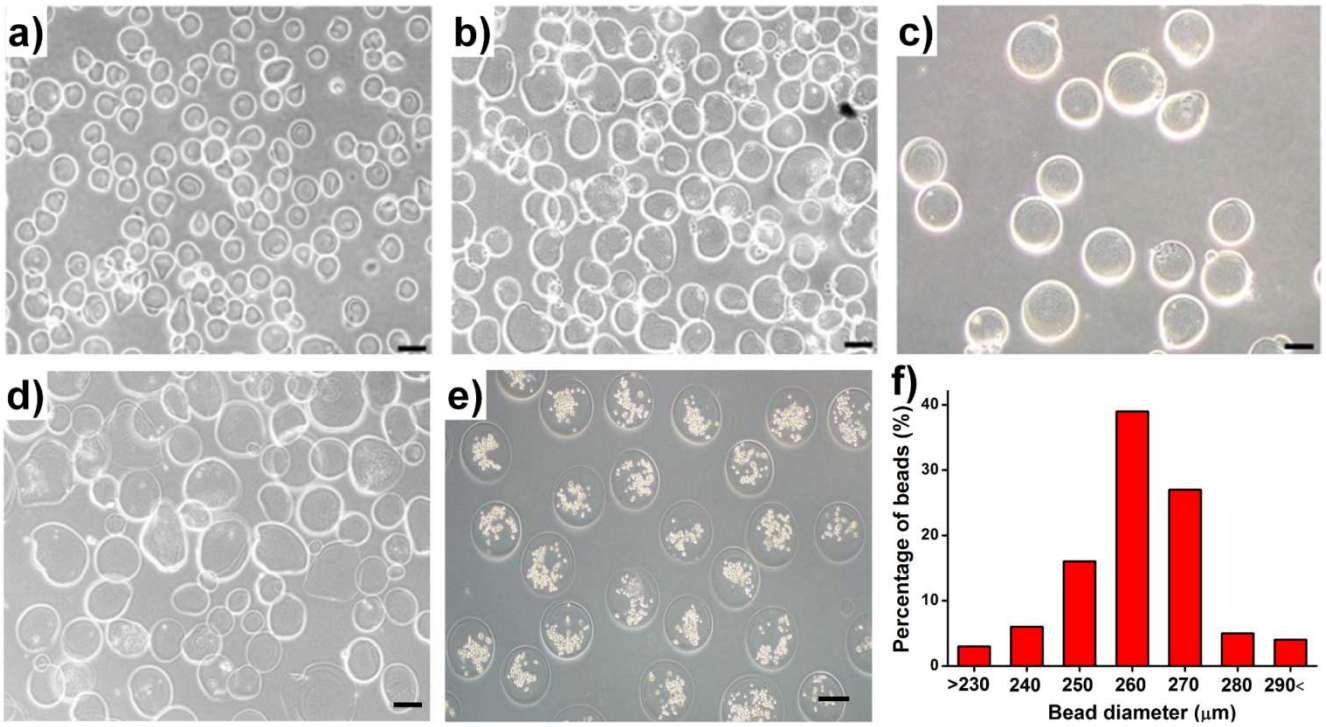

Fig. 4

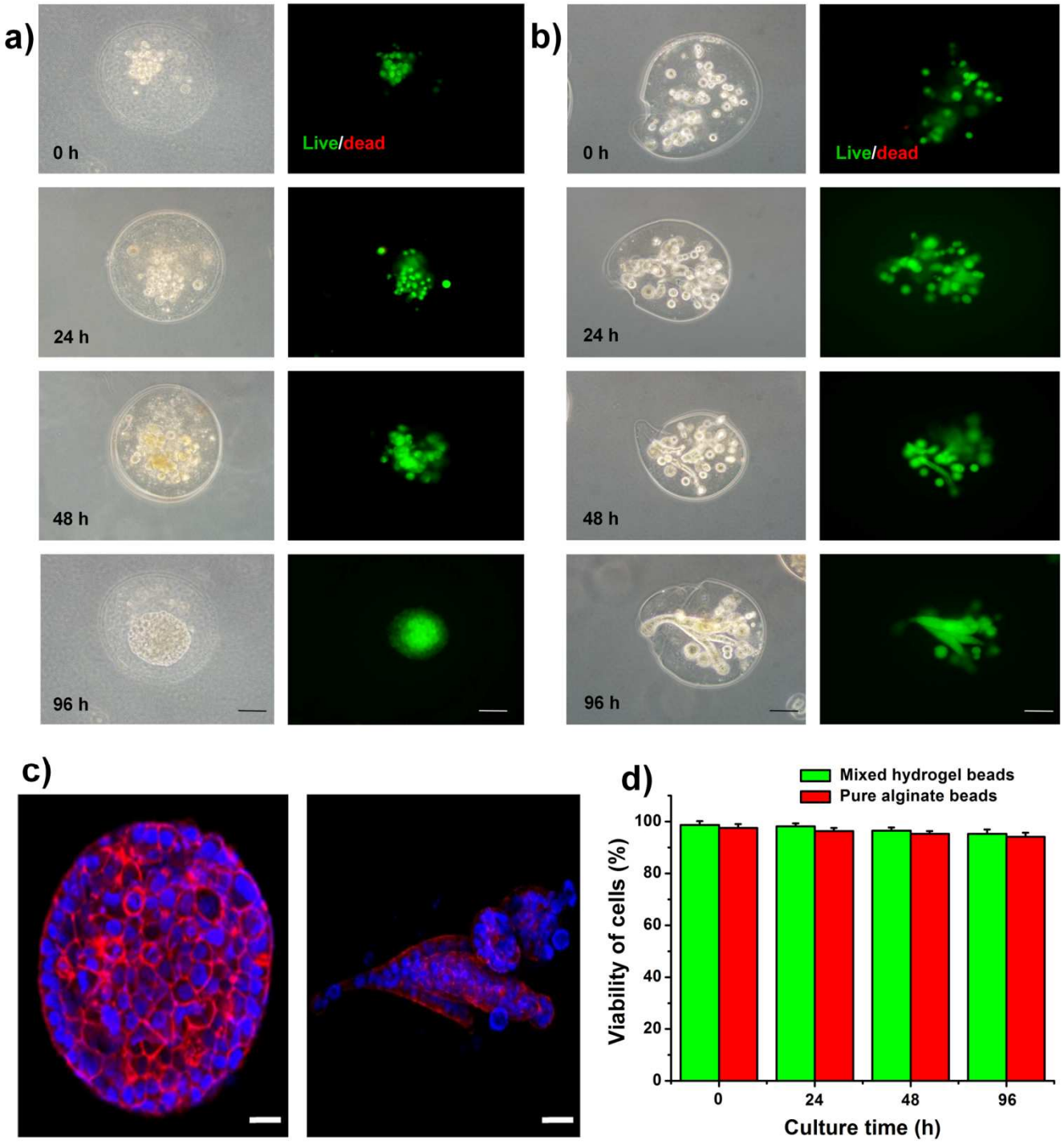

Fig. 5

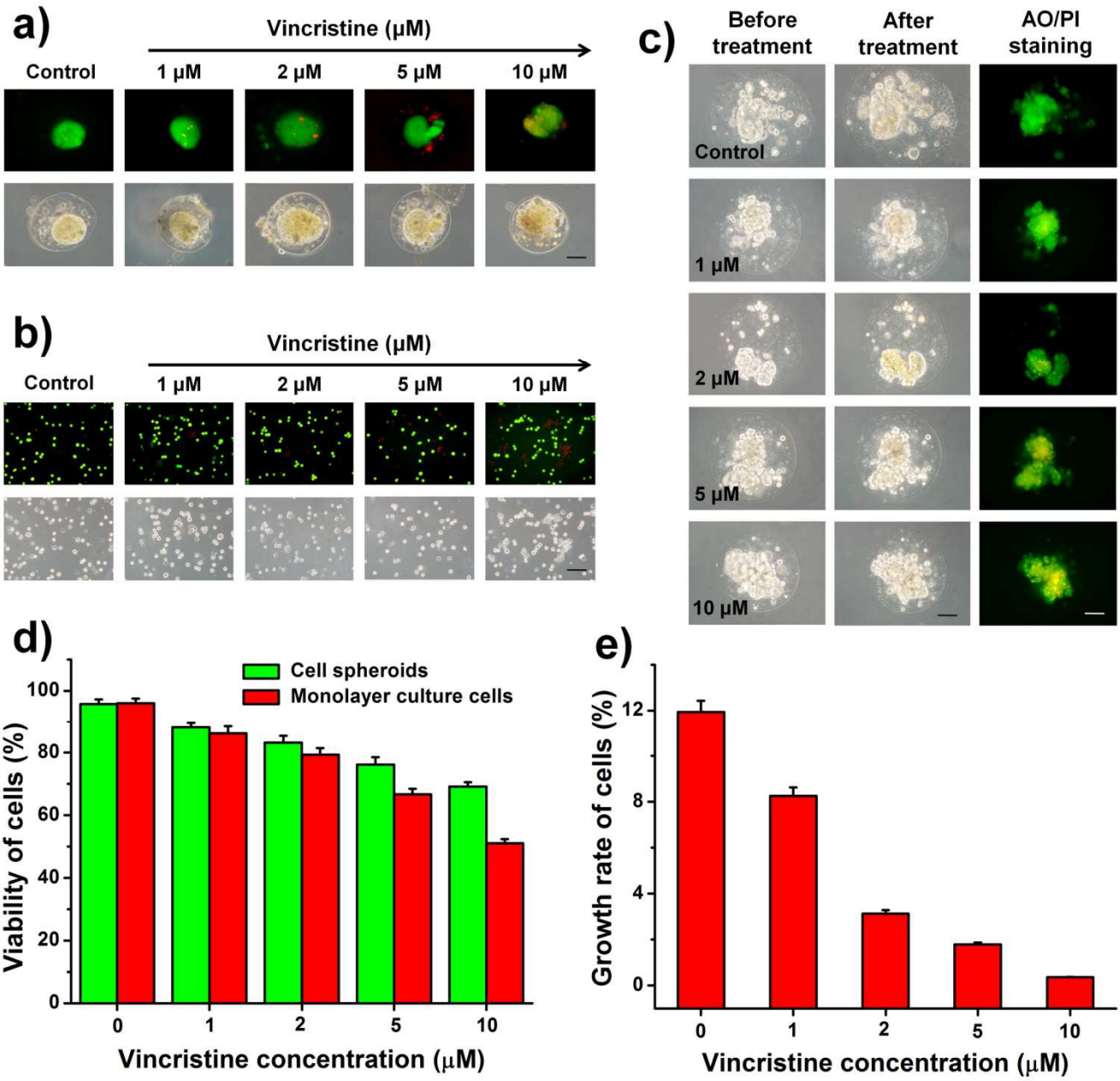

Fig. 6

Graphical abstract

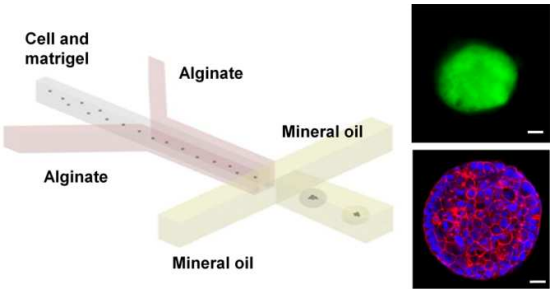

A microfluidic method was developed for the formation of tumor spheroids using alginate and matrigel mixed hydrogel beads.